A general relation for contact stiffness including adhesion in indentation analysis

Pin Lu,[a] Yong L. Foo, Lu Shen, Davy W.C. Cheong, and Sean J. O'Shea
*Institute of Materials Research and Engineering, Agency for Science, Technology and Research (A*STAR), Singapore 117602*

(Received 14 January 2011; accepted 8 April 2011)

The Maugis–Barquins (MB) solutions for the adhesive contact between an axisymmetric indenter and an elastic half-space are modified by incorporating the interfacial energy defined by the real area of contact. With the modified MB solutions, general relations for contact stiffness including adhesive effects in indentation analysis are derived. Numerical calculations showed that the difference in expected stiffness for the modified MB model compared to the standard MB results can be significant at low loads of interest in atomic force microscopy measurements and also for indentation tests at high load if the interfacial energy is large ($\sim$0.1 J/m^2) and the material is soft (Young's modulus $\leq$100 MPa).

I. INTRODUCTION

A goal of indentation characterization is to extract the elastic modulus and indentation hardness of materials from load-displacement curves. Given that the basic parameter measured in indentation testing to extract hardness and elasticity is the contact stiffness, the relationship between the contact stiffness and the elastic modulus is of key importance. On the basis of the Sneddon contact solutions without adhesion, Oliver and Pharr[1,2] derived simple contact stiffness relations for a general axisymmetric indenter and hence developed an improved method to measure the hardness and elastic modulus of a material from indentation load-displacement data. The relations have been widely used in indentation characterization.

In the Oliver–Pharr analysis,[1,2] the effect of adhesion between the indenter and the material surface is not taken into consideration. The influence of adhesion between contacting surfaces becomes important for smooth surfaces and for biological or soft materials.[3–5] The incorporation of adhesion in elastic contact was addressed in the Johnson–Kendall–Roberts (JKR) model,[6] which is now generally used for contact problems with compliant materials. A review of JKR and other adhesive contact models can be found in Ref. 7. Subsequently, on the basis of physical relationships between the adhesive contact and the fracture mechanics, Maugis and Barquins[8–10] extended the JKR model using the Sneddon solutions[11] to adhesive contacts of general axisymmetric indenters on an elastic half-space. The Maugis–Barquins (MB) solutions can be applied to obtain general relations including adhesive effects for indentation analysis, and results for some specific indenter geometries[12,13,17] have been obtained.

The adhesive contact surface in the MB solutions[8–10] is defined by the projected area of contact between the indenter and the surface (see Fig. 1), not the real area of contact between the surfaces. This difference is not a concern for a flat-ended indenter as in this case, the MB solutions are exact. The MB solutions are also a good approximation for a spherical indenter of large radius.[6] However, errors may arise for some types of indenter, for example, a sharp conical indenter, in which the difference between the real contact surface and the projected area could be considerable. Therefore, the MB solutions for an adhesive contact should be modified to consider real contact area in the definition of adhesive energy. Such corrections have been undertaken, but only for specific indenter geometries.[12,13] In this article, a more general solution is presented for the contact stiffness of any axisymmetric indenter, and it incorporates adhesion and the real area of interface contact.

The article is arranged as follows. The Sneddon[11] and MB[8–10] solutions are briefly reviewed first, as these are the basis of the derivations. The MB solutions are then modified by introducing the interfacial energy defined by the real contact area. The modified MB solutions are then used to derive general relations for contact stiffness including adhesion. Finally, for application in indentation analysis, the results of contact stiffness for some specific geometries are obtained.

II. REVIEW OF PREVIOUS DESCRIPTIONS

A. Review of Sneddon solutions for the axisymmetric Boussinesq problem

Consider a normal frictionless contact with no adhesion between a rigid axisymmetric indenter with an arbitrary profile of $z = f(r)$ and an elastic half-space as shown in Fig. 1(a). The shape function can also be written in the form $z = f(r/a)$, in which a is the radius of the

[a]Address all correspondence to this author.
e-mail: lup@imre.a-star.edu.sg
DOI: 10.1557/jmr.2011.132

 © Materials Research Society 2011

https://doi.org/10.1557/jmr.2011.132 Published online by Cambridge University Press

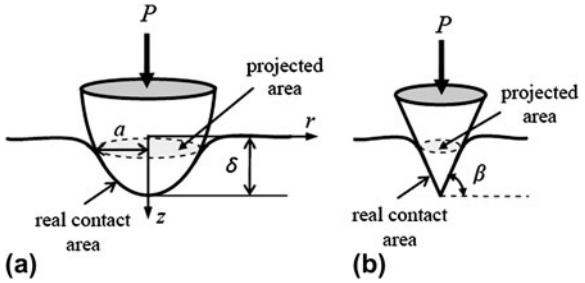


FIG. 1. (a) Schematic view of the profile formed between a rigid axisymmetric indenter and the surface of an elastic half-space. The real contact area usually differs from the projected contact area. (b) Definition of the angle β for a rigid conical indenter.

projected circular area of the contact surface. The mixed boundary conditions of the contact problem in a cylindrical coordinate system at $z = 0$ can be described as[10,11]:

$$u_z(r,0) = \delta - f(r/a), \quad 0 \le r \le a \quad ,$$

$$\sigma_{zz}(r,0) = 0, \quad r > a \quad ,$$

$$\tau_{rz}(r,0) = 0, \quad 0 \le r \le \infty \quad ,$$

where δ is the penetration depth of the indenter tip, $\sigma_{zz}(r,0)$ the distribution of pressure, $\tau_{rz}(r,0)$ the distribution of shear stress, and $u_z(r,0)$ the vertical displacement. The indenter profile shape function should satisfy $f(0) = 0$. On the basis of the method of Hankel transforms, concise and elegant solutions for the problem were obtained by Sneddon.[11] The main results of the solutions are[10,11]

$$\delta = \int_0^1 \frac{f'(x)}{\sqrt{1-x^2}}\,dx + \frac{\pi}{2}\chi(1) \quad , \tag{1}$$

$$P = \pi a E^* \int_0^1 \chi(t)\,dt = 2aE^*\left(\delta - \int_0^1 \frac{xf(x)}{\sqrt{1-x^2}}\,dx\right) \quad , \tag{2}$$

$$\sigma_{zz}(r,0) = -\frac{E^*}{2a}\left(\frac{\chi(1)}{\sqrt{1-r^2a^2}} - \int_{r/a}^1 \frac{\chi'(t)}{\sqrt{t^2-r^2/a^2}}\,dt\right) \quad , \quad r < a \quad , \tag{3}$$

$$u_z(r,0) = \int_0^1 \frac{\chi(t)}{\sqrt{r^2/a^2 - t^2}}\,dt = \chi(1)\sin^{-1}\frac{a}{r} - \int_0^1 \chi'(t)\sin^{-1}\frac{at}{r}\,dt \quad , \quad r > a \quad . \tag{4}$$

where P is the load, which must be applied to achieve the penetration δ, and the function $\chi(t)$ is defined by

$$\chi(t) = \frac{2}{\pi}\left(\delta - \frac{d}{dt}\int_0^t \frac{xf(x)}{\sqrt{t^2-x^2}}\,dx\right) = \frac{2}{\pi}\left(\delta - t\int_0^t \frac{f'(x)}{\sqrt{t^2-x^2}}\,dx\right) \quad , \tag{5}$$

and $E^* = E/(1-\nu^2)$ is the effective Young's modulus.

In Sneddon solutions,[11] the parameter $\chi(1)$ is set to be zero to eliminate the singular stress of $\sigma_{zz}(r,0)$ at the edge of the contact, which gives the general solutions for the nonadhesion contact model (denoted by the subscript S) as

$$\delta_S = \int_0^1 \frac{f'(x)}{\sqrt{1-x^2}}\,dx \quad , \tag{6}$$

$$P_S = 2aE^*\left(\delta_S - \int_0^1 \frac{xf(x)}{\sqrt{1-x^2}}\,dx\right) \quad . \tag{7}$$

On the basis of the general solutions, the corresponding results for some specific indenter shapes can be obtained.[11] In particular, Pharr et al.[1] verified that the contact stiffness S_S based on the nonadhesion contact model is independent of indenter geometry, that is,

$$S_S = \frac{dP_S}{d\delta_S} = 2aE^* = \frac{2E^*}{\sqrt{\pi}}\sqrt{A_p} \quad , \tag{8}$$

where $A_p = \pi a^2$ is the projected circular area of the contact surface.

B. Review of MB solutions for adhesive contact

Johnson, Kendall, and Roberts[6] (JKR) studied adhesive contact between a spherical indenter and an elastic half-space. It was shown by Maugis and Barquins[8,9] that the JKR solutions[6] can be viewed as a Griffith's model of fracture with the edge of the contact being a crack tip. By applying Sneddon solutions,[11] Maugis and Barquins successfully extended the JKR model to adhesive contacts of general axisymmetric indenters on an elastic half-space.

In the MB solutions, the total energy U_T of the system is $U_T = U_E + U_M + U_S$,[6,14] where U_E and U_M are the stored elastic energy and the mechanical potential energy change due to the applied load, respectively, and U_S is the interfacial energy, expressed as $U_S = -\gamma A_p$, where γ is the interfacial energy per unit area.[14,15] Solutions for adhesive contact can be obtained under the equilibrium condition $dU_T = (G_p - \gamma)dA_p = 0$, where

$$G_p = \frac{\partial(U_E + U_M)}{\partial A_p} \quad , \tag{9}$$

is the energy release rate with the dimensions of energy per unit projected area.[8–10] When adhesion is present, the

https://doi.org/10.1557/jmr.2011.132 Published online by Cambridge University Press

parameter $\chi(1)$ in the Sneddon solutions can be nonzero, implying that singular contact stresses arise at the contact edge. Therefore, there is a connection between the parameter $\chi(1)$ and the stress intensity factor K_I in fracture mechanics, which can be determined from Eq. (3) as[8–10,17] $K_I = -\frac{E^*}{2}\sqrt{\frac{\pi}{a}}\chi(1)$. Further, the relationship between the strain energy release rate G_p and the stress intensity factor K_I is given by[16] $G_p = \frac{1}{2E^*}K_I^2$. This establishes a link between G_p and $\chi(1)$. Let P_1 be the apparent load that, if $\chi(1) = 0$, gives the same contact radius as that observed under load P with $\chi(1) \neq 0$ ($P_1 > P$).[6,8–10] Using Eqs. (1) and (2),

$$P_1 = 2aE^*\left[\int_0^1 \frac{f'(x)}{\sqrt{1-x^2}} - \mathrm{d}x \int_0^1 \frac{xf(x)}{\sqrt{1-x^2}}\mathrm{d}x\right] \quad , \quad (10)$$

and from Eqs. (2) and (10),

$$P_1 - P = -\pi a E^* \chi(1) \quad . \quad (11)$$

The energy release rate G_p can thus be expressed as

$$G_p = \frac{1}{8\pi a^3 E^*}(P_1 - P)^2 \quad , \quad (12)$$

and the load P in MB adhesive contact solutions can be obtained by the equilibrium condition $G_p = \gamma$.[8–10,14]

III. MODIFICATION OF MB SOLUTIONS

A. Solutions incorporating real area of contact

The interfacial energy in both JKR and MB solutions[6,8–10] is defined by the projected circular area $A_p = \pi a^2$ of the interfacial contact area as shown in Fig. 1. Below, the MB adhesive contact solutions are modified by incorporating the interfacial energy using the real interfacial contact area.

When real contact area is considered, the interfacial energy U_S is written as

$$U_S = -\gamma A \quad , \quad (13)$$

where A is the real contact area of the two surfaces, rather than the projected circular area A_p. Solutions for adhesive contact can be obtained under the condition $dU_T = (G-\gamma)^* dA = 0$, where $G = \partial(U_E + U_M)/\partial A$ is the energy release rate per unit contact area. However, to make use of the formulas adopted in the Maugis and Barquins derivations,[8–10] the condition $dU_T = 0$ can also be expressed as

$$dU_T = \left(G_p - \gamma\frac{\partial A}{\partial A_p}\right)dA = 0 \quad , \quad (14)$$

where G_p is given in Eq. (9). For an axisymmetric indenter with profile shape function $z = f(r)$, we have $dA = 2\pi r\sqrt{1 + [f'(r)]^2}dr$ and $dA_p = 2\pi r dr$. The ratio $\partial A/\partial A_p$ at $r = a$ thus can be expressed as $\partial A/\partial A_p = \sqrt{1 + [f'(r)|_{r=a}]^2}$. Therefore, the equilibrium condition [Eq. (14)] is equivalent to

$$G_p = \kappa_a \gamma \quad , \quad (15)$$

where κ_a is the indenter geometry parameter given by

$$\kappa_a = \sqrt{1 + [f'(r)|_{r=a}]^2} \quad . \quad (16)$$

Therefore, for modeling real interfacial contact area, the balance condition to determine the adhesive contact solutions is modified to Eq. (15), rather than $G_p = \gamma$. It is noted that the relations reduce to the MB model if $\kappa_a = 1$, that is, if the projected circular area A_p is used in Eq.(13).

By substituting Eq. (12) into the new equilibrium condition [Eq. (15)], the modified MB relationship between P and a at equilibrium is given by

$$P = P_1 - \sqrt{8\pi E^* a^3 \kappa_a \gamma} \quad . \quad (17)$$

This relation can be simplified to

$$P = P_1 - P_\gamma \quad , \quad (18)$$

where

$$P_\gamma = \sqrt{8\pi E^* a^3 \kappa_a \gamma} \quad , \quad (19)$$

is the adhesion force, and P_1 is given by Eq. (10).

By considering the real adhesive contact area, the value of the parameter $\chi(1)$ is modified by Eqs. (11) and (17) as $\chi(1) = -\sqrt{\frac{8a\kappa_a\gamma}{\pi E^*}}$. By substituting this value into the general solution Eq. (1), the modified penetration depth of the indenter is

$$\delta = \int_0^1 \frac{f'(x)}{\sqrt{1-x^2}}\mathrm{d}x - \sqrt{\frac{2\pi a\kappa_a\gamma}{E^*}} = \delta_1 - \delta_\gamma \quad , \quad (20)$$

with

$$\delta_1 = \int_0^1 \frac{f'(x)}{\sqrt{1-x^2}}\mathrm{d}x, \quad \delta_\gamma = \sqrt{\frac{2\pi a\kappa_a\gamma}{E^*}} \quad , \quad (21)$$

where δ_1 is the indenter tip displacement in nonadhesion contact, and δ_γ is the indenter tip displacement due to adhesion effects.

Comparing the relations obtained in this section, we observe that the MB solutions[8–10] are modified by the parameter κ_a introduced into the interfacial energy related terms, that is, P_γ in Eq. (19) and δ_γ in Eq. (21). For $\kappa_a = 1$, the relations reduce to the MB solutions,[8–10] and with no adhesion ($\gamma = 0$), δ and P reduce to the Sneddon solutions Eqs. (6) and (7).

https://doi.org/10.1557/jmr.2011.132 Published online by Cambridge University Press

B. Solutions for contact stiffness including adhesion effects

In this section, the general relation of contact stiffness including adhesion is derived on the basis of the modified MB solutions. The contact stiffness in indentation is defined as $S = \mathrm{d}P/\mathrm{d}\delta$. Noting that the parameter κ_a in Eq. (16) is a function of the radius a of the projected circular area, Eq. (17) gives

$$\frac{\mathrm{d}P}{\mathrm{d}a} = \frac{\mathrm{d}P_1}{\mathrm{d}a} - 3\sqrt{2\pi a E^* \kappa_a \gamma} - \sqrt{\frac{2\pi a^3 E^* \gamma}{\kappa_a}}\frac{\mathrm{d}\kappa_a}{\mathrm{d}a} \quad , \quad (22)$$

in which $\mathrm{d}P_1/\mathrm{d}a$ can be determined from Eq. (10). Following the treatment of Pharr et al.[1]

$$\frac{\mathrm{d}P_1}{\mathrm{d}a} = 2aE^*\frac{\mathrm{d}\delta_1}{\mathrm{d}a} \quad , \quad (23)$$

where

$$\frac{\mathrm{d}\delta_1}{\mathrm{d}a} = \frac{\mathrm{d}}{\mathrm{d}a}\int_0^1 \frac{f'(x)}{\sqrt{1-x^2}}\mathrm{d}x \quad . \quad (24)$$

From Eqs. (20) and (21), $\mathrm{d}\delta_1/\mathrm{d}a$ can also be expressed as

$$\frac{\mathrm{d}\delta_1}{\mathrm{d}a} = \frac{\mathrm{d}\delta}{\mathrm{d}a} + \frac{\mathrm{d}\delta_\gamma}{\mathrm{d}a} = \frac{\mathrm{d}\delta}{\mathrm{d}a} + \sqrt{\frac{\pi\kappa_a\gamma}{2aE^*}} + \sqrt{\frac{\pi a\gamma}{2E^*\kappa_a}}\frac{\mathrm{d}\kappa_a}{\mathrm{d}a} \quad . \quad (25)$$

By substituting Eqs. (25) and (23) into Eq. (22), we obtain

$$\frac{\mathrm{d}P}{\mathrm{d}a} = 2aE^*\frac{\mathrm{d}\delta}{\mathrm{d}a} - \sqrt{8\pi E^* a\kappa_a\gamma} \quad . \quad (26)$$

Hence, the general relation of contact stiffness including adhesion effects can be found from Eqs. (26) and (25) as

$$S = \frac{\mathrm{d}P}{\mathrm{d}\delta} = \mathrm{d}P/\mathrm{d}a \Big/ \mathrm{d}\delta/\mathrm{d}a = 2aE^* - \frac{\sqrt{8\pi E^* a\kappa_a\gamma}}{\mathrm{d}\delta_1/\mathrm{d}a - \sqrt{\pi\kappa_a\gamma/2aE^*} - \sqrt{\pi a\gamma/2E^*\kappa_a}\mathrm{d}\kappa_a/\mathrm{d}a} \quad , \quad (27)$$

where $\mathrm{d}\delta_1/\mathrm{d}a$ is given by Eq. (24). Note that both δ_1 and κ_a, and hence the contact stiffness, depend on the indenter geometry $f(x)$. Eq. (27) can also be written as

$$S = S_1 - S_\gamma \quad , \quad (28)$$

with

$$S_1 = 2aE^*,$$

$$S_\gamma = \frac{\sqrt{8\pi aE^*\kappa_a\gamma}}{\mathrm{d}\delta_1/\mathrm{d}a - \sqrt{\pi\kappa_a\gamma/2aE^*} - \sqrt{\pi a\gamma/2\kappa_a E^*}\mathrm{d}\kappa_a/\mathrm{d}a} \quad . \quad (29)$$

Again, with no adhesion ($S_\gamma = 0$), Eq. (28) reduces to the Sneddon contact solution Eq. (8), and for $\kappa_a = 1$, $S_\gamma = \sqrt{8\pi aE^*\gamma}/(\mathrm{d}\delta_1/\mathrm{d}a - \sqrt{\pi\gamma/2aE^*})$, which is the MB solution.[8–10]

IV. RESULTS FOR SPECIAL CASES

In this section, we apply the general solutions obtained to some specific indenter geometries.

For a flat-ended cylindrical indenter with radius a, the contact area is the circular area πa^2. Since the shape function of the flat indenter is $f(r/a)=0$, we have $\kappa_a = 1$ and $P_1 = 0$. The pull-off (adhesive) force and the corresponding displacement induced thus can be determined from Eqs. (17) and (20) as

$$\delta = -\sqrt{\frac{2\pi a\gamma}{E^*}} \quad , \quad (30)$$

$$P = -\sqrt{8\pi E^* a^3\gamma} = 2aE^*\delta \quad . \quad (31)$$

These results are identical to those calculated by Kendall.[18,19] Since the radius a is constant for a flat-ended cylindrical indenter, the contact stiffness $\mathrm{d}P/\mathrm{d}\delta$ is

$$S = 2aE^* \quad , \quad (32)$$

which is independent of the interfacial surface energy γ.

For a spherical indenter with $a \ll R$, where R is the radius of the sphere, the shape function can be approximately expressed by an ellipsoidal function as[10]

$$f(r/a) = \frac{a^2(r/a)^2}{2R}, \quad a \ll R \quad . \quad (33)$$

Substituting Eq. (33) into Eq. (16) gives

$$\kappa_a = \sqrt{1 + (a/R)^2} \approx 1, \quad \frac{\mathrm{d}\kappa_a}{\mathrm{d}a} \approx 0 \quad . \quad (34)$$

The penetration, contact force, and contact stiffness obtained from Eqs. (20), (17), and (27) give the well-known JKR solutions,[6,7,20]

$$\delta = \frac{a^2}{R} - \sqrt{\frac{2\pi a\gamma}{E^*}} \quad , \quad (35)$$

$$P = \frac{4E^* a^3}{3R} - \sqrt{8\pi a^3 E^*\gamma} \quad , \quad (36)$$

$$S = 2aE^* - \frac{\sqrt{8\pi aE^*\gamma}}{2a/R - \sqrt{\pi\gamma/2aE^*}} \quad . \quad (37)$$

https://doi.org/10.1557/jmr.2011.132 Published online by Cambridge University Press

With no adhesion ($\gamma = 0$), δ and P in Eqs. (35) and (37) reduce to the Hertz contact solutions.[21,7]

For a conical indenter with a semivertical angle β [see Fig. 1(b)], the surface profile is[10]

$$f(r/a) = (r/a)a\tan\beta \quad . \tag{38}$$

Substituting Eq. (38) into Eq. (16) gives

$$\kappa_a = \sqrt{1 + (f'(r)|_{r=a})^2} = 1/\cos\beta, \quad \frac{d\kappa_a}{da} = 0 \quad , \tag{39}$$

and inserting Eqs. (38) and (39) into Eqs. (20), (17), and (27) gives the penetration, contact force, and contact stiffness,

$$\delta = \frac{\pi a}{2}\tan\beta - \sqrt{\frac{2\pi a\gamma}{E^*\cos\beta}} \quad , \tag{40}$$

$$P = \frac{\pi}{2}a^2E^*\tan\beta - \sqrt{\frac{8\pi a^3E^*\gamma}{\cos\beta}} \quad , \tag{41}$$

$$S = 2aE^* - \frac{\sqrt{8\pi aE^*\gamma/\cos\beta}}{\pi(\tan\beta)/2 - \sqrt{\pi\gamma/(2aE^*\cos\beta)}} \quad . \tag{42}$$

The results [Eqs. (40)–(42)] are identical to those obtained by Yang[12] for the case of frictionless contact with a conical indenter, also using the real contact area for interfacial energy. The only difference here is that a simpler derivation is followed and the solutions are general for axisymmetric indenters.

It is apparent from Eqs. (40)–(42) that for a sharp conical indenter, such as an atomic force microscopy (AFM) tip, cos β can be much smaller than one and the differences between model solutions may be significant. Figures 2–5 give an indication of the magnitude of such differences by showing numerical comparisons between the MB solutions and the newly modified MB solutions for a rigid conical indenter. To cross-check the results with those of Yang,[12] in the examples chosen, the half-space material studied is poly-dimethyl-siloxane with material properties of $E = 24.5$ MPa, $\nu = 0.5$, and yield stress is ~2.5 MPa. Figure 2 compares load P versus radius of projected area by an indenter with $\beta = 60°$ and $\gamma = 0.028$ J/m^2 for the different models. There are two regimes of most interest. For indentation measurement of hardness and elasticity, the unloading response at high applied load [Fig. 2(a)] is required.[22] For the modified MB solution, a larger radius evolves compared to the MB solution for the same peak load. The behavior at low loads [Fig. 2(b)] describes a regime of interest in AFM experiments, and

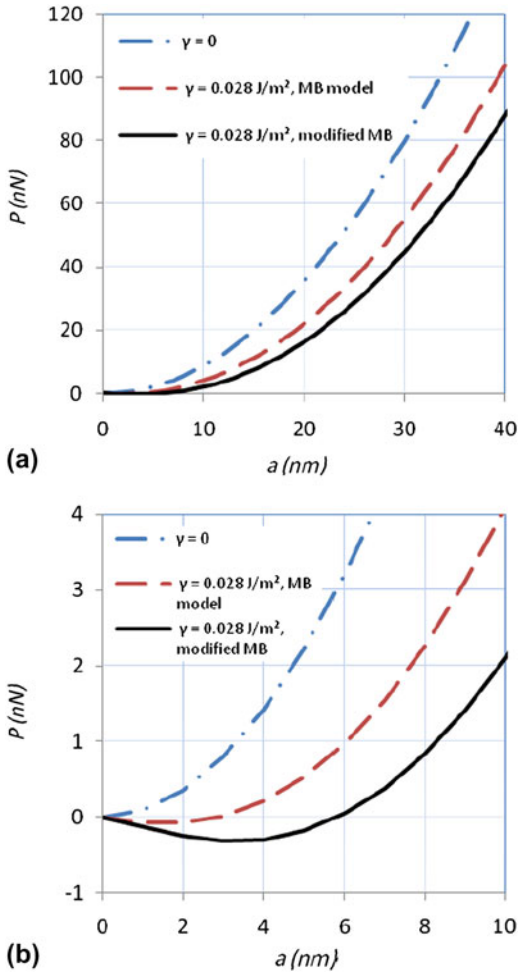


FIG. 2. (a) Variation of radius (a) of projected area with load (P) for a rigid conical indenter ($\beta = 60°$) for the Sneddon ($\gamma = 0$), the MB ($\gamma = 0.028$ J/m^2), and the modified MB ($\gamma = 0.028$ J/m^2) models. The half-space material parameters are $E = 24.5$ MPa and $\nu = 0.5$, similar to poly-dimethyl-siloxane. (b) A close up of the low load region of (a).

here a large difference is observed between models, with a deeper and broader adhesion region for the modified MB solution. This is not surprising given that the area used in the interfacial energy term for the modified MB theory is larger in comparison to the projected area of the standard MB solution. The data can be plotted in the more familiar form of load versus indentation depth (Fig. 3), from which similar conclusions in the low- and high-load regimes can be drawn. Figure 3(b) highlights again the large influence of the interfacial energy term γ at low loads, with increasingly large differences between the models as γ increases from 0.028 to 0.1 J/m^2; however, one should always note that the error in γ itself is uncertain because of the difficulty in determining γ experimentally.[23]

The material elasticity and hardness are calculated from the measured stiffness at high load.[22] Accordingly, Figures 4 and 5 compare the stiffness for the MB and

https://doi.org/10.1557/jmr.2011.132 Published online by Cambridge University Press

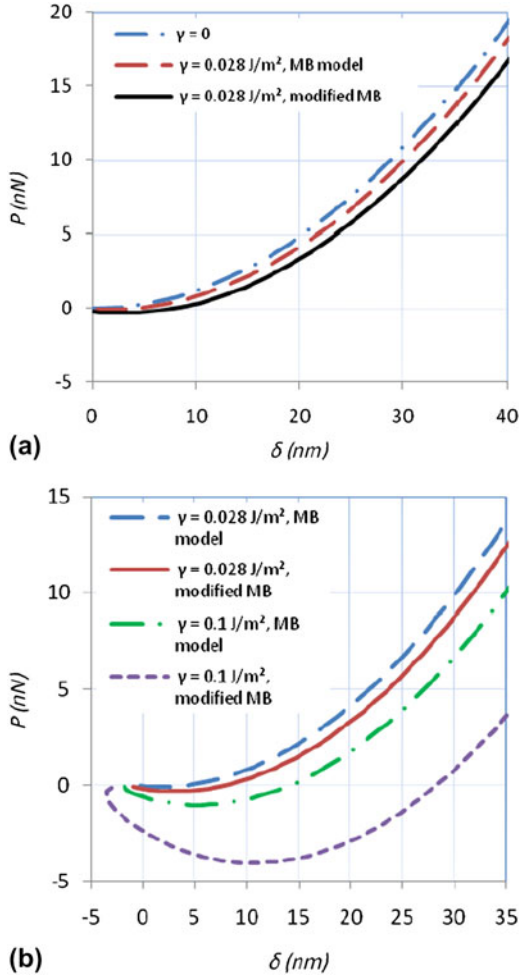


FIG. 3. (a) Variation of indentation depth (δ) with load (P) for a rigid conical indenter (β = 60°) for the Sneddon (γ = 0), the MB (γ = 0.028 J/m^2), and the modified MB (γ =0.028 J/m^2) models. The half-space material parameters are E = 24.5 MPa and ν = 0.5, similar to poly-dimethyl-siloxane. (b) A close up of the low-load region of (a) with additional data shown for the case γ = 0.1 J/m^2.

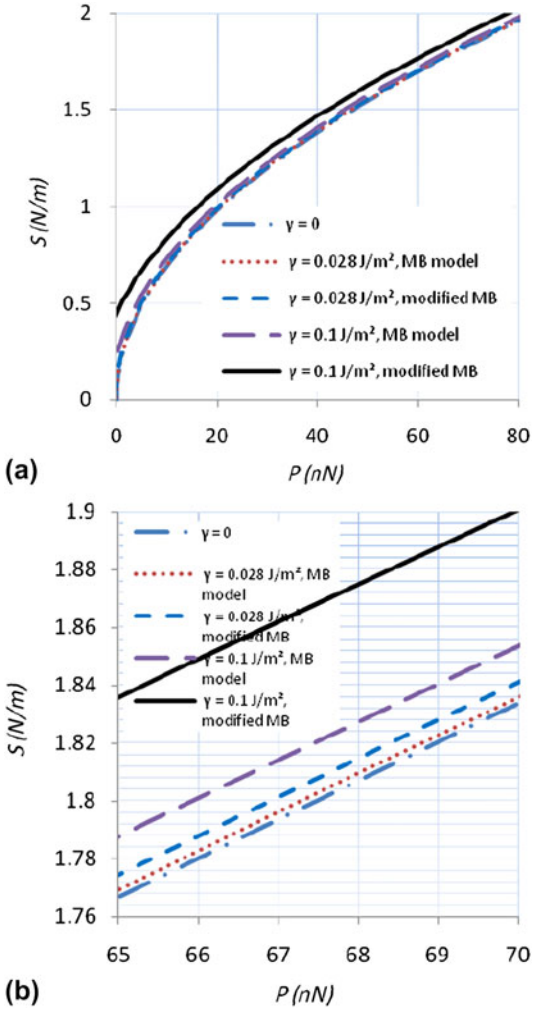


FIG. 4. (a) Variation of contact stiffness (S) with load (P) for a rigid conical indenter (β = 60°) for the Sneddon (γ = 0), the MB, and the modified MB models. The half-space material parameters are E = 24.5 MPa and ν = 0.5, similar to poly-dimethyl-siloxane. Two values of interfacial energy are shown (γ =0.028 J/m^2 and γ = 0.1 J/m^2). (b) A close up of the high-load region of (a) showing differences in contact stiffness between the models, which, in turn, influence the calculation of material hardness and elasticity.

modified MB models. The stiffness changes nonlinearly as a function of load [Fig. 4(a)] with the numerical difference between the two models increasing as the load decreases. At high load [Fig. 4(b)], the curves show approximately constant difference *at fixed load* between the MB and the modified MB models of ~1.4% for γ = 0.028 J/m^2 and ~2.7% for γ = 0.1 J/m^2. The corresponding high-load data *for a fixed penetration depth* (Fig. 5) shows differences between the models of ~1.7% for γ = 0.028 J/m^2 and ~5.6% for γ = 0.1 J/m^2.

Similar numerical calculations using E = 24.5 MPa and ν = 0.5 were undertaken for a shallower conical indenter with β = 19.7, that is, a Berkovich's type analogue. As expected, as β becomes small, the difference between the MB and the modified MB results decreased to a negligibly small value at high applied load (a ~0.15% difference in contact stiffness for γ = 0.1 J/m^2). Large differences between the models can exist at loads near zero (a ~5% difference in contact stiffness for γ = 0.1 J/m^2), but in practice the Berkovich indenter would not be used in the low-load regime. Finally, simulations for a hard material with E = 20 GPa (data not presented) show the difference between the models, which is negligible, irrespective of the value of γ. Thus, for a conical indenter at fixed load or fixed penetration depth, the differences between the MB and modified MB models for high-load indentation experiments are only significant (within a few percent) if γ is large (~0.1 J/m^2), β is large (~60°), and E is small (≤100 MPa).

https://doi.org/10.1557/jmr.2011.132 Published online by Cambridge University Press

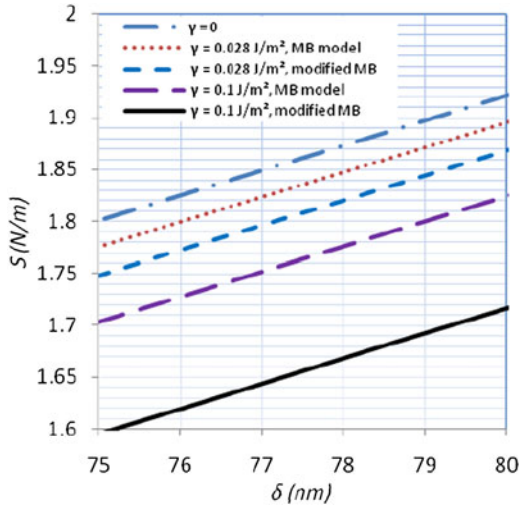


FIG. 5. Variation of contact stiffness (S) with indentation depth (δ) in the high load regime for a rigid conical indenter ($\beta = 60°$) for the Sneddon ($\gamma = 0$), the MB, and the modified MB models. The half-space material parameters are $E = 24.5$ MPa and $\nu = 0.5$, similar to polydimethyl-siloxane. Two values of interfacial energy are shown ($\gamma = 0.028$ J/m^2 and $\gamma = 0.1$ J/m^2).

V. CONCLUDING REMARKS

The MB solutions[8–10] for the adhesive contact between an axisymmetric indenter and an elastic half-space were modified to incorporate the interfacial energy defined by the real contact area. The solutions obtained are general for axisymmetric shaped indenters. Hence, the contact stiffness including adhesive effects was derived for use in indentation analysis and relations for some known indenter geometries (flat, sphere, and cone) shown. Numerical calculations showed that the difference in expected stiffness for the modified MB model compared to the standard MB results can be significant at low loads of interest in AFM measurements and is a ~3% effect for conical indenters at high loads if γ is large (~0.1 J/m^2) and the material is soft ($E \leq 100$ MPa).

The advantage of the general solutions given is that adhesive contact for any axisymmetric indenter can be analyzed. For comparison purposes, only known results for the flat, spherical, and conical indenter geometries have been presented. However, adhesive contact solutions for other axisymmetric indenters such as paraboloid or ellipsoid of revolution can be obtained in a similar manner. The general solutions may also be applied to study the importance of adhesion and indenter tip shape at low loads[24] and to extract mechanical properties of soft materials or nanostructures probed by AFM with different tip shapes.[25,26] Finally, the general solutions can be used to investigate the application range of various approximate solutions. For example, the JKR model for a spherical indenter is based on the assumption $a \ll R$. However, when a is comparable to R, the exact shape function $f(r/a)$ should be used to obtain the general adhesive contact solutions. These applications will be studied in a subsequent paper.

REFERENCES

1. G.M. Pharr, W.C. Oliver, and F.R. Brotzen: On the generality of the relationship among contact stiffness, contact area, and elastic modulus during indentation. *J. Mater. Res.* **7**, 613 (1992).
2. W.C. Oliver and G.M. Pharr: An improved technique for determining hardness and elastic-modulus using load and displacement sensing indentation experiments. *J. Mater. Res.* **7**, 1564 (1992).
3. U.D. Schwarz: A generalized analytical model for the elastic deformation of an adhesive contact between a sphere and a flat surface. *J. Colloid Interface Sci.* **261**, 99 (2003).
4. D.M. Ebenstein and L.A. Pruitt: Nanoindentation of biological materials. *Nano Today*. **1**, 26 (2006).
5. Y.F. Cao, D.H. Yang, and W. Soboyejoy: Nanoindentation method for determining the initial contact and adhesion characteristics of soft polydimethylsiloxane. *J. Mater. Res.* **20**, 2004 (2005).
6. K.L. Johnson, K. Kendall, and A.D. Roberts: Surface energy and the contact of elastic solids. *Proc. R. Soc. London, Ser. A* **324**, 301 (1971).
7. E. Barthel: Adhesive elastic contacts: JKR and more. *J. Phys. D: Appl. Phys.* **41**, 163001 (2008).
8. D. Maugis and M. Barquins: Adhesive contact of sectionally smooth-ended punches on elastic half-spaces: Theory and experiment. *J. Phys. D: Appl. Phys.* **16**, 1843 (1983).
9. D. Maugis: Adhesion of spheres: The JKR-DMT transition using a Dugdale model. *J. Colloid Interface Sci.* **150**, 243 (1992).
10. D. Maugis: *Contact, Adhesion and Rupture of Elastic Solids* (Springer, Heidelberg, 2000).
11. I.N. Sneddon: The relation between load and penetration in the axisymmetric Boussinesq problem for a punch of arbitrary profile. *Int. J. Eng. Sci.* **3**, 47 (1965).
12. F.Q. Yang: Effect of adhesion energy on the contact stiffness in nanoindentation. *J. Mater. Res.* **21**, 2683 (2006).
13. L. Sirghi and F. Rossi: Adhesion and elasticity in nanoscale indentation. *Appl. Phys. Lett.* **89**, 243118 (2006).
14. D. Maugis and M. Barquins: Fracture mechanics and the adherence of viscoelastic bodies. *J. Phys. D: Appl. Phys.* **11**, 1989 (1978).
15. D. Tabor: Surface forces and surface interactions. *J. Colloid Interface Sci.* **58**, 2 (1977).
16. B. Lawn: *Fracture of Brittle Solids*, 2nd ed. (Cambridge University Press, Cambridge, 1993).
17. D. Vallet and M. Barquins: Adhesive contact and kinetics of adherence if a rigid conical punch on an elastic half-space (natural rubber). *Int. J. Adhes. Adhes.* **22**, 41 (2002).
18. K. Kendall: The adhesion and surface energy of elastic solids. *J. Phys. D: Appl. Phys.* **4**, 1186 (1971).
19. F.Q. Yang: Thickness effect on the indentation of an elastic layer. *Mater. Sci. Eng., A* **358**, 226 (2003).
20. F.Q. Yang: Adhesive contact between a rigid axisymmetric indenter and an incompressible elastic thin film. *J. Phys. D: Appl. Phys.* **35**, 2614 (2002).
21. H. Hertz: On the contact of elastic solids, in *Miscellaneous Papers by Heinrich Hertz*, English translated by D.E. Jones and G.A. Schott (Macmillan and Co., Ltd., new York, 1896), p. 146.
22. A.C. Fischer-Cripps: Review of analysis and interpretation of nanoindentation test data. *Surf. Coat. Tech.* **200**, 4153 (2006).

https://doi.org/10.1557/jmr.2011.132 Published online by Cambridge University Press

23. A. Olah and G.J. Vancso: Characterization of adhesion at solid surfaces: Development of an adhesion-testing device. *Eur. Polym. J.* **41**, 2803 (2005).
24. A.M. Korsunsky: The influence of punch blunting on the elastic indentation response. *J. Strain Anal. Eng. Des.* **36**, 391 (2001).
25. E.K. Dimitriadis, F. Horkay, J. Maresca, B. Kachar, and R.S. Chadwick: Determination of elastic moduli of thin layers of soft material using the atomic force microscope. *Biophys. J.* **82**, 2798 (2002).
26. J.R. Withers and D.E. Aston: Nanomechanical measurements with AFM in the elastic limit. *Adv. Colloid Interface Sci.* **120**, 57 (2006).

https://doi.org/10.1557/jmr.2011.132 Published online by Cambridge University Press